Solid-state Characterization of the HIV Protease Inhibitor

Yongae Kim* and **Aeri Kim†**

Dept. of Chemistry, Hankuk University of Foreign Studies, San 89, Mohyun, Yongin 449-791, Korea
†LG LS, 104-1, Moonji-dong, Yusong-gu, Daejeon 305-380, Korea
Received August 13, 2002

The LB71350, (3S, 4R)-Epoxy-(5S)-[[N-(1-methylethoxy)carbonyl]-3-(methylsulfonyl)-L-valinyl]amino]-N-[2-methyl-(1R)-[(phenyl)carbonyl]propyl-6-phenylhexanamide, is a novel HIV protease inhibitor. Its equilibrium solubility at room temperature was less than 40 μg/mL. It was speculated that the low aqueous solubility might be due to the high crystalline lattice energy resulting from intermolecular hydrogen bonds. The present study was carried out to learn the solid-state characteristics of LB71350 using analytical methods such as NMR, FT-IR and XRD. ^{13}C Solid-state NMR, solution NMR, and FT-IR spectra of the various solid forms of LB71350 were used to identify the conformation and structure of the solid forms. The chemical shifts of ^{13}C solid-state NMR spectra suggest that the crystalline form might have 3 intermolecular hydrogen bondings between monomers.

Key Words : HIV protease inhibitor, ^{13}C solid-state NMR, Solution NMR, FT-IR, Chemical shift

Introduction

Solid form characterization of a drug substance is important from chemical development point of view because its crystallinity will influence the yield, rate, and quality of the crystallization. From pharmaceutical development point of view, its hygroscopicity, stability, solubility and processibility should be considered significantly as well as pharmacokinetic aspects and toxicological effects.[1-3] Solubility and dissolution rate of a drug substance is particularly important to achieve good absorption after oral administration. A novel HIV protease inhibitor LB71350, (3S,4R)-Epoxy-(5S)-[[N-(1-methylethoxy)carbonyl]-3-(methylsulfonyl)-L-valinyl]-amino]-N-[2-methyl-(1R)-[(phenyl)carbonyl]propyl-6-phenyl-hexanamide, is poorly water soluble. Its equilibrium solubility at room temperature was less than 40 μg/mL.[1] It was speculated that the low aqueous solubility might be due to the high crystalline lattice energy resulting from intermolecular hydrogen bonds. Figure 1 shows the computer-simulated structure of LB71350 monomer. A crystalline form designated as Form **I** was produced from pilot lab synthesis. Early preclinical studies were done using a cosolvent mixture
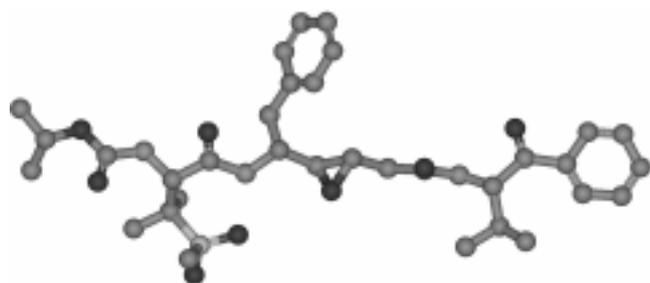

Figure 1. The 3D model structure of LB71350, (3S,4R)-Epoxy-(5S)-[[N-(1-methylethoxy) carbonyl]-3-(methylsulfonyl)-L-valinyl] amino]-N-[2-methyl-(1R)-[(phenyl) carbonyl] propyl-6-phenyl hexanamide.

such as propylene glycol/ethanol/Tween 80 to overcome its poor aqueous solubility. The present study was carried out to learn the solid state characteristics of LB71350 using analytical methods such as solid-state ^{13}C NMR and liquid state ^{13}C NMR, FT-IR and XRD. We compare the spectral data of crystalline Form **I** and amorphous solid form of LB71350 to identify the structural information and polymorphology.

Experimental Methods

Preparation of Crystalline Form I. 150 mg of LB71350 was dissolved in 2 mL ethylacetate. This solution was left at room temperature with a loosely fitted cover in the dark. After 7 days solid was collected and used without further drying.

Preparation of Amorphous Solid Form. 150 mg of LB71350 was dissolved in 5 mL ethanol and the solvent was removed by rotary evaporation in a 45 °C water bath. The residue was dried in a vacuum oven overnight. The collected solid was grounded and passed through a 62 μm sieve before analysis.

XRD Studies. XRD powder patterns were recorded using a Rigaku Geigerflex IIIC. Samples were mounted on 0.2 mm cavity sample holders. Typical continuous scan was done using the following conditions; scan type: standard, Axis: $2\theta/\theta$, Start: 3°, Stop: 35°, Scan speed: 5°/min, Sampling interval: 0.03, Data type: counts/sec, Voltage: 35 kV, Current: 20 mA.

FTIR Spectroscopy. Samples were prepared by KBr pellet method. Spectra were obtained with the FT-IR spectrophotometer (BIO-RAD, FTS-60A) using the following conditions: Wavenumber; 4000-400 cm^{-1}, Resolution number; 4 cm^{-1}, Number of scan; 16.

Solid-State NMR Spectroscopy. [13]C solid-state nmr spectra were measured at 75.4 MHz on a Bruker DSX 300 MHz NMR Spectrometer with static magnetic field strengths of

7.05 T, using a standard double bearing probe head. Samples were placed into 4 mm zirconia rotor. Spectra were recorded using (CP)MASDD and several spectral editing techniques (CPPI, CPMOSL, CPMOSPISLTB, etc) for assignment[5-9] with 4-15 KHz different spinning rate and recorded under room temperature. Magic angle was adjusted using ^{79}Br resonance of KBr at first, and the ^{13}C resonance of adaman-tane and glycine were used to assure the accurate setting. The chemical shifts were referenced to carbonyl chemical shift of glycine at 176.03 ppm. Each chemical shift was assigned using spectral editing techniques and verified by liquid state nmr spectra.

Liquid-State NMR Spectroscopy. ^{13}C Liquid state NMR measurements were performed at 75.4 MHz on a Bruker ARX 300 MHz NMR Spectrometer with the static magnetic field strengths of 7.05 T, using a standard carbon 5 mm probe head at room temperature. Several experiments of ^{1}H-NMR, ^{13}C-NMR, DEPT90, DEPT135, COSY, and HETCOR were used to assign peaks of LB71350. Experiments were done in CDCl$_3$ at room temperature. Bruker DMX 600 MHz NMR spectrometer was also used to confirm the data.

Results and Discussion

XRD and FT-IR Spectroscopy. Rapid removal of solvent from ethanol solution of LB71350 resulted in amorphous solid with a XRD pattern typical for amorphous solid (Figure 2-1). In contrast, crystallization from ethylacetate gave crystalline form **I** which showed sharp peaks indicating good crystallinity (Figure 2-2). FT-IR spectra of crystalline and amorphous solids are shown in Figure 3. Their finger print regions are identical. But distinctive differences are noted in the -CO- and -NH- band regions. While the peaks of -CO- (at 1669.7 cm^{-1}) and of -NH- (at 3344.7 cm^{-1}) in the spectrum of the amorphous solid are rather broad (Figure 3-1), those in the crystalline form **I** have two sharp split peaks (Figure 3-2). This peak splitting indicates two different
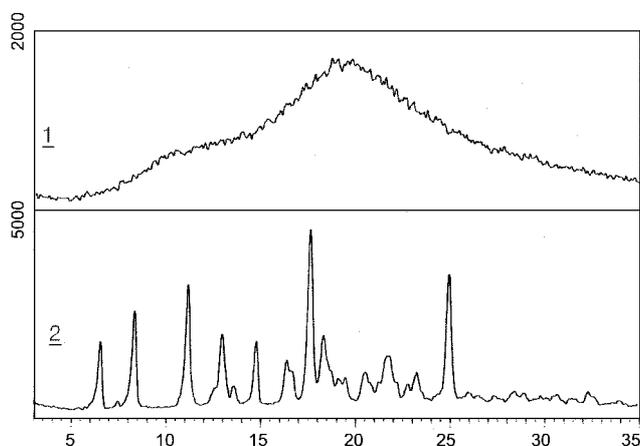

Figure 2. XRD powder patterns of amorphous solid form and crystalline solid form of LB71350 A XRD pattern of amorphous solid form of LB71350 is typical for amorphous solid. In contrast, crystalline form I which showed sharp peaks indicating good crystallinity. 1) Amorphous solid form 2) Crystalline solid Form **I**.
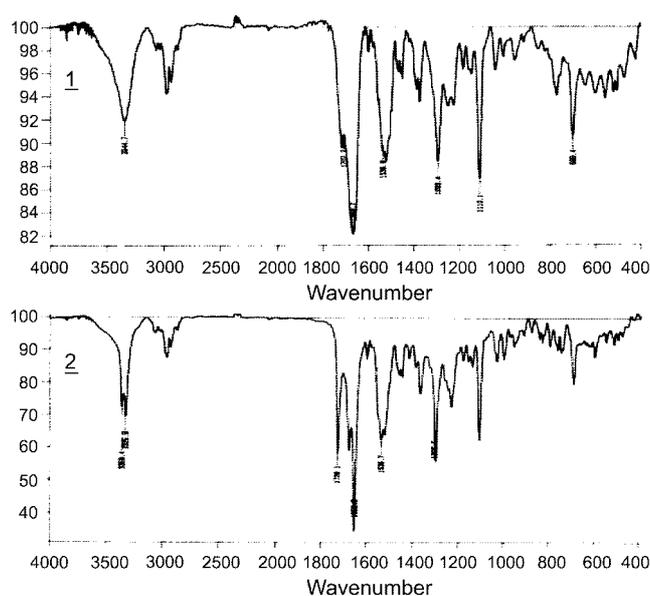

Figure 3. FT-IR Spectra of LB71350. Their finger print regions are identical. But distinctive differences are noted in the -CO- (at 1669.7 cm^{-1}) and of -NH- (at 3344.7 cm^{-1}) band regions. 1) Amorphous solid form 2) Crystalline solid Form **I**.

populations of peptide bonds in the crystal of LB71350. IR peak position changes depending on H-bonding, which induces peak shift to lower wave numbers. For example, CO stretching peak in amide bond appears at ~1685 cm^{-1} when free and at ~1660 cm^{-1} when H-bonded.[10] In the solid form study of dirithromycin, -CO-peak of amorphous form showed a single resonance whereas the crystalline form I showed two peaks.[11] These two peaks in the crystalline form were assigned to H-bonded and non-H-bonded carbonyl groups in this form. Their solid state NMR results confirmed the suggestion from IR spectra. Similarly, the two peaks in the -CO- region of the FTIR spectra of the crystalline form **I** of LB71350 in the present study can also be assigned to one from the functional groups participating in intermolecular H-bonding (1652.8 cm^{-1}) are and to another from those with no H-bonding (1728.1 cm^{-1}). Solid state NMR study below demonstrates further how each -CO- carbons differ in terms of H-bonding. For -NH- bond region, all 3 -NH- groups participate in H-bonding in the crystalline form I according to the results of the solid state NMR below. Therefore the peak splitting in the crystalline form **I** of -NH- region in the IR spectrum must be due to the subtle difference in the environment among different -NH-groups including H-bonding distance.

Solid-State NMR Spectroscopy. The ^{13}C solid-state NMR spectra of an amorphous powder form show overall broad peak pattern in Figure 4. This suggests that the amorphous powder form have been successfully made. Even though all chemical shift resonances are very broad, each chemical shift of ^{13}C solid state NMR is almost the same as that of liquid state NMR spectra.

Unlike the spectra of amorphous powder form, each ^{13}C chemical shift of the crystalline form shows sharp resonance,
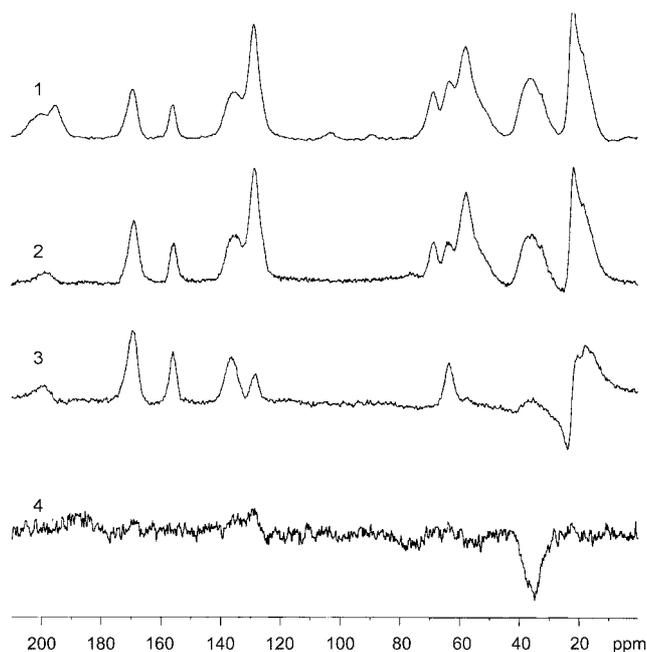
Figure 4. Solid-state ^{13}C NMR Spectra of LB71350 amorphous form show overall broad peak pattern. It suggests that the amorphous powder form have been successfully made. Pulse programs used are as below. 1) CP-MAS at 5KHz spin rate which show all resonace including spinning side band. 2) CP-MAS-TOSS at 4 KHz spin rate which show all resonance without spinning side band. 3) CP-MAS-TOSS-DELAY at 4 KHz spin rate which show methyl carbon and quarternary carbon. 4) CP-MOSPISL-TOSS at 4 KHz spin rate which show negative methylene only.

Figure 5. Solid-state ^{13}C NMR spectra of LB71350 crystalline form shows sharp resonance, which is dominated by intramolecular conformational effects and morphology. Pulse programs used are as below. 1) CPMAS at 5KHz spin rate 2) CPMASTOSS at 4 KHz spin rate 3) CPMASTOSSDELAY at 4 KHz spin rate 4) CPMOSPISLTOSS at 4 KHz spin rate

which are dominated by intramolecular conformational effects and morphology in Figure 5. The spectrum of crystalline Form **I** is almost like that of liquid state NMR. Figure 5-3 shows quaternary carbon only and Figure 5-4 shows negative methylene carbon only. All ^{13}C chemical shifts are assigned using solid-state NMR spectral editing technique[5-17] and confirmed by liquid state NMR spectra. Table 1 shows ^{13}C chemical shifts of all carbon in crystalline state of LB71350. The C35 carbonyl peak of crystalline form shifts to downfield approximately 5 ppm than that of amorphous state. C9 and C31 carbonyl peaks shift to downfield around 1 ppm than that of amorphous state, but C5 carbonyl peak of crystalline form shifts to upfield around 2 ppm than that of amorphous state. These chemical shifts suggest that the crystalline form might have a possibility to have 3 intermolecular hydrogen bondings between monomers. C35, C9, and C31 carbonyl groups have hydrogen bond with other monomer but not C5 carbonyl group. C35 carbonyl group possibly has hydrogen bond with NH beside C5 carbonyl group so the chemical shift of C5 carbonyl group move to upfield about 2 ppm. Therefore the intermolecular hydrogen bonding with other monomer is more favorable than intramolecular hydrogen bonding within monomer. NH group beside C9 and C31 carbonyl group have another hydrogen bonding with C31 and C9 carbonyl groups in order so that the chemical shift difference is only about 1 ppm. In conclusion, crystalline form of LB71350 might have a linear
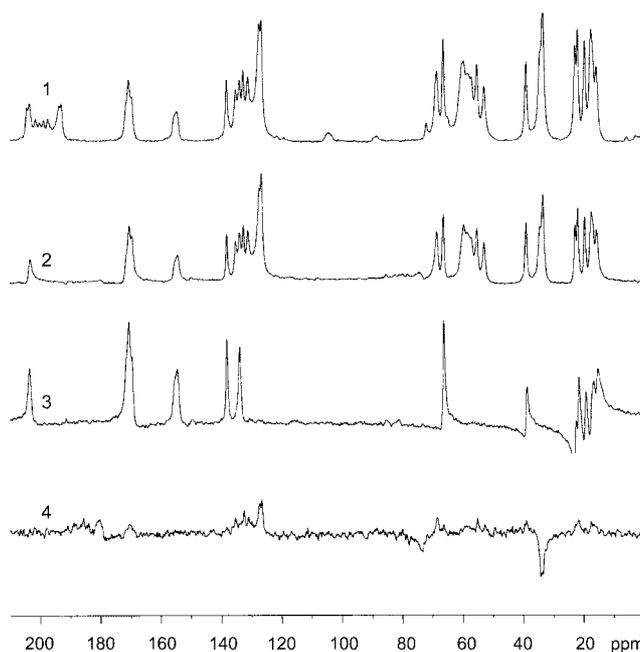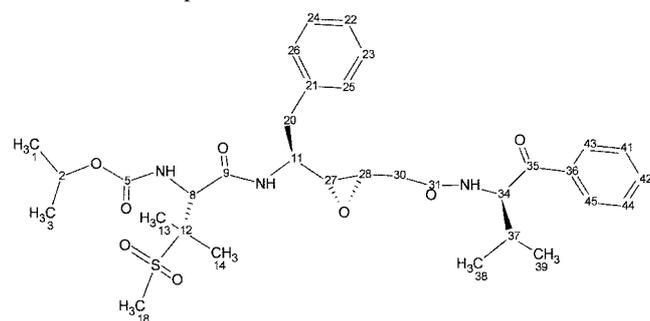
β-sheet structure and possibly have intermolecular hydrogen bonding between monomer. These results are verified by unpublished results from computer simulation.[18]

Therefore, ^{13}C solid-state NMR spectra of the crystalline powder form also confirmed the intermolecular H-bonding in the crystalline Form **I**. And ^{13}C chemical shift and structure of the crystalline powder form are induced by an intermolecular conformational effects rather than intramolecular conformation effects like amorphous powder state. Figure 6 shows the model of 3 intermolecular hydrogen bondings of the crystalline form of the LB71350. It is most likely that the C35 carbonyl group is hydrogen-bonded to the first -NH group in a neighboring molecule.
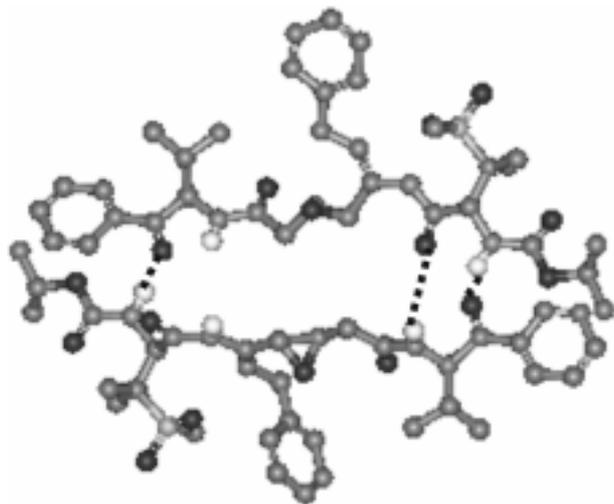
Figure 7 shows the solid-state and liquid-state ^{13}C NMR spectra of crystalline form and amorphous form of LB71350. Because of all carbons are under very rapid motion in liquid state, all carbon chemical shifts are induced by an intramolecular conformation effects that means all resonance show average position. Therefore, there is no chemical shift difference between crystalline form and amorphous form in liquid state NMR.
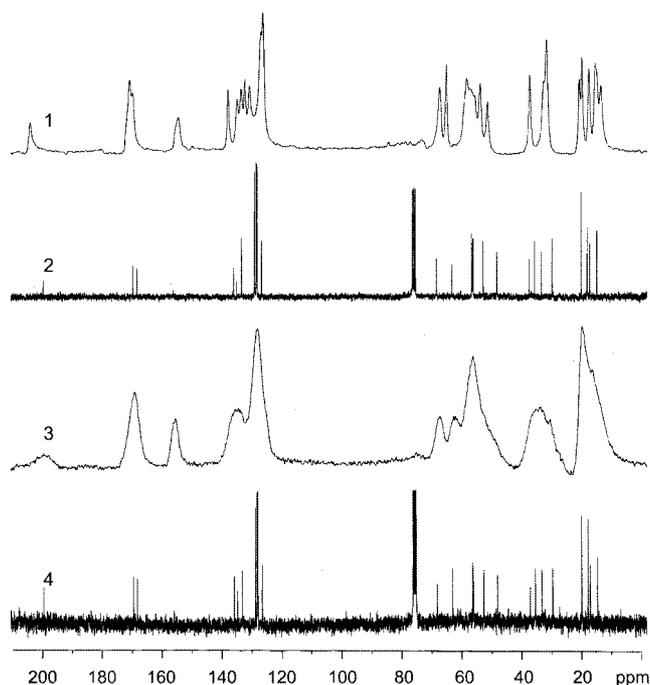
Conclusions

Structure and morphology of the crystalline Form **I** and amorphous form of LB71350 is readily identified using ^{13}C solid-state NMR spectroscopy along with XRD and IR. The structural information and morphology of the crystalline powder and amorphous powder are well defined and distinguished. Both NMR and IR data provided the evidence

Table 1. ^{13}C chemical shifts of LB71350 crystallline form from solid-state NMR spectra

Carbon number	Chemical Shift (ppm)	Carbon number	Chemical Shift (ppm)
1 & 3	12-22	**23-26**	128-130
2	69.5	**27**	54.2
5	155	**28**	57.5
8	57.7	**30**	35
9	168	**31**	169
11	50	**34**	58
12	64	**35**	199
13-14	17-22	**36**	135
18	37	**37**	32
20	39	**38-39**	17-22
21	136	**41 & 43-45**	128-130
22	127	**42**	133

Figure 6. The model structure of three intermolecular hydrogen bondings of the crystalline form of the LB71350. ^{13}C NMR chemical shifts suggest that the crystalline form might have a possibility to have 3 intermolecular hydrogen bondings between monomers.

that peptide bonds of LB71350 participate in intermolecular hydrogen bonds in crystalline Form **I**. Although single crystal X-ray data are required for unequivocal structure determination, the present study demonstrates that solid state NMR and FTIR can provide useful information on solid state characteristics when single crystal is not available. Further study is in progress to examine and characterize

Figure 7. ^{13}C NMR Spectra of LB71350 1) Solid-state NMR Spectrum of crystalline solid Form **I** 2) Liquid state NMR spectrum of crystalline solid Form **I** 3) Solid-state NMR spectrum of amorphous solid form 4) Liquid state NMR spectrum of amorphous solid form.

other crystalline forms of LB71350.

References

1. Byrn, S.; Pfeiffer, R.; Ganey, M.; Hoiberg, C.; Poochikian, G. *Pharm. Res.* **1995**, *12*, 945.
2. Jeong, Y. N.; Seo, M. K.; Lee, S. H.; Choi, Y. J.; Kim, I. C.; Lee, Y. H. *Pharm. Res.* **1996**, *13*, s-486.
3. Grunenberg, A.; Keil, B.; Henck, J. O. *Int. J. of Pharmaceutics* **1995**, *118*, 11.
4. Gao, P. *Pharm. Res.* **1996**, *13*, 1095.
5. Middleton, D. A.; Le Duff, C. S.; Berst, F.; Reid, D. G. *J. of Pharm. Sci.* **1997**, *86*, 1400.
6. Opella, S. J.; Frey, M. H. *J. Am. Chem. Soc.* **1979**, *101*, 5854.
7. Hu, J. Z.; Wu, X.; Yang, N.; Li, L.; Ye, C.; Qin, K. *Solid State NMR* **1996**, *6*, 187.
8. Wu, X.; Burns, S. T.; Zilm, K. W. *J. Magn. Res. Ser A* **1994**, *111*, 29.
9. Wu, X.; Zilm, K. W. *J. Magn. Res. Ser A* **1993**, *102*, 205.
10. Pretsch, *et al.*, *Tables of Spectral Data for Structure Determination of Organic Compounds*, 2nd Ed.; Springer-Verlag: 1989.
11. Stephensen, G. A.; Stowell, J. G.; Toma, P. H.; Dorman, D. E.; Greene, J. R.; Byrn, S. R. *J. Am. Chem. Soc.* **1994**, *116*, 5766.
12. Wu, X. *et al. J. Magn. Res. Ser A* **1993**, *104*, 119.
13. Lee, J. H.; Gi, U. S.; Kim, J. H.; Kim, Y.; Kim, S. H.; Oh, J. S.; Min, B. C. *Bull. Korean Chem. Soc.* **2001**, *22*, 925.
14. Kim, Y. *Biochem. News* 2001, *21*, 253.
15. Kim, Y.; Kim, A. *ENC (Experimental Nuclear Magnetic Resonance Conference*; 2001; p 95.
16. Kim, Y. *J. Basic Sci. HUFS* **2001**, *12*, 69.
17. Kim, Y. *ENC (Experimental Nuclear Magnetic Resonance Conference)*; 2002; p 187.
18. Unpublished results from computer simulation, from Dr. Rho SungGu, LG CI.